KYBERNETIKA — VOLUME *48* (2012), NUMBER 2, PAGES 223–241

CONTROL OF THE UNDERACTUATED MECHANICAL SYSTEMS USING NATURAL MOTION

Zdeněk Neusser and Michael Valášek

The paper deals with the control of underactuated mechanical systems between equilibrium positions across the singular positions. The considered mechanical systems are in the gravity field. The goal is to find feasible trajectory connecting the equilibrium positions that can be the basis of the system control. Such trajectory can be stabilized around both equilibrium positions and due to the gravity forces the mechanical system overcomes the singular positions. This altogether constitutes the control between the equilibrium positions. The procedure is demonstrated on the different inverse pendulum mechanisms.

Keywords: underactuated systems, nonlinear control, mechanical systems

Classification: 70E55, 93C10, 93B60

1. INTRODUCTION

This study deals with the control of mechanical systems moving in the gravity field with fewer actuators than degrees of freedom, so called underactuated systems. In the applications further described in this paper the concept of underactuated systems can be defined by this relation, although the more precise definition should be based on the number of blocks in the Brunovsky canonical form [9]. It is investigated the control of underactuated mechanical systems between equilibrium positions passing through singularity positions in the gravity field. These systems are in this area uncontrollable by considered NQR control ([6, 11]) with zero velocity, in particular it is the swing-up of pendubot and of pendulum on the cart (called also cart-pole system, see [2]). The controllability is calculated from the controllability matrix composed of A and B matrices derived at each time step and evaluating its rank. These studied mechanisms can be controlled in their equilibrium positions (see [4]), but between these equilibrium states there are always singularity points. The main goal is to determine the behavior of the actuator(s) to get them through the singularities. To move the mechanism through this region or even trajectory tracking (see [1]) is a challenging task.

These problems have been already investigated by many authors. There is used in [5] the method adding the actuators to the underactuated joints and running the swing-up motion with optimization minimizing the action of the added actuators. Partly stable controllers derived using the dynamic model of the manipulator in order to employ them under an optimal switching sequence is presented in [7]. Energy based approach

used in the design of stabilizing controllers is in the book [2]. The friction forces are used in energy control strategy in [3]. Another approach is to use exact input-output linearization within certain submanifold (direction) in which the system is controllable and the zero-dynamics is stable.

Work [10] presents the way of the feedforward control strategy combined with input-output linearization. After this transformation the system acquires new input variables that are suitable to control the actuated part together with the underactuated one. However, the system can be controlled by this new input only if the input functions are from the certain admissible class of functions. One way of finding such admissible class of functions is cyclic control described in [8] as periodic invariant (with respect to the actuated variables) functions without details.

This paper describes another way of finding suitable admissible functions for the control of the underactuated systems between equilibrium positions across singularity areas in the gravity field. These suitable admissible functions are based on the inversion of the so-called natural motion or on the reuse of specific knowledge gained from these natural motions. Shortly, the natural motion is a motion of the system without control.

2. UNDERACTUATED MECHANICAL SYSTEMS

As mentioned above, there are some uncontrollable states between equilibrium states. Standard control algorithm fails to get the mechanism through these singular positions to reach the upper position. Situation is indicated in the Figure 1.

In this figure on the left-hand side the pendubot is described in the upper unstable equilibrium position, then in the middle singular position and in the lower stable equilibrium position. On the right-hand side the same three positions are depicted for the cart-pole system. The middle part of the Figure 1 describes the general path from equilibrium position 1 across the singular positions to the equilibrium position 2. The singular positions are in the middle row of the Figure 1 for zero velocities. Equilibrium positions can be successfully controlled by some type of nonlinear control. In this paper a nonlinear quadratic regulator is used (NQR or SDRE, see [6] and [11]). The main goal is to move the mechanism from one equilibrium point to another one and successfully pass through the singular positions. Singular positions are positions where the control strategy fails and controllability matrix has lower rank than the number of states. Here the control strategy of NQR is used. This control strategy is capable to stabilize the system in the large area around the equilibrium positions. However, the computation of this control based on the solution of Riccatti equation completely fails at the singular positions, see Figure 1. The controllability of the investigated systems is in general judged using the controllability matrix within the NQR algorithm, besides the direct analysis of the equations of motion of systems under consideration at the singular positions described in the equations (28) and (34).

To construct such control strategy, that is able to take the system across the uncontrollable area, it is necessary to gain some knowledge about the behavior of the mechanism when passing through such singularities. It is possible to get this information within so-called natural motion described further.

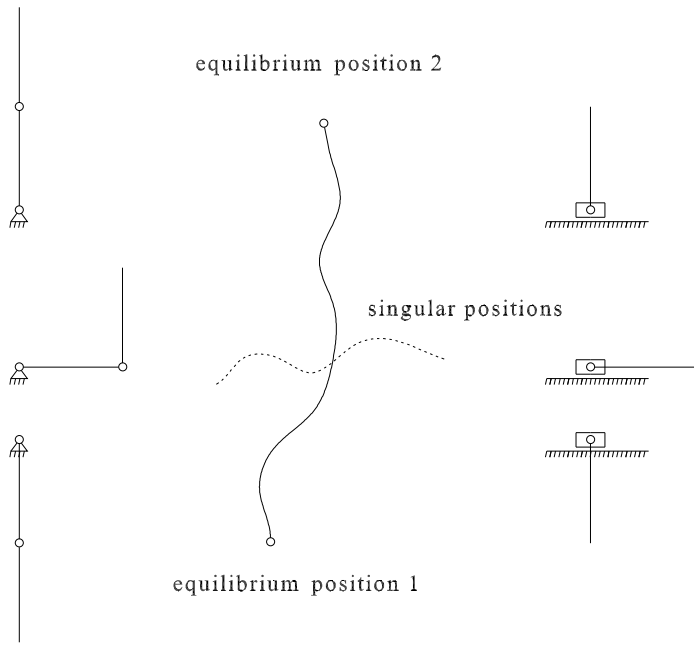

Fig. 1. Stable positions with pointed singular configurations.

3. EXACT INPUT-OUTPUT FEEDBACK LINEARIZATION

The linearization is derived in [10]. A modified version is used and described further in this section. Let us consider a dynamic system

$$M(q) \cdot \ddot{q}(t) = F(q, \dot{q}) + B(q) \cdot u(t) \tag{1}$$

where matrix $M[n \times n]$ is a inertia matrix, $q[n \times 1]$ are coordinates describing the system, $\dot{q}$ and $\ddot{q}$ their derivatives, $F[n \times 1]$ is matrix containing forces dependent on velocities and external forces besides control inputs, $B[n \times k]$ is control input distribution matrix and the vector $u[k \times 1]$, $k < n$ contains the control inputs.

The goal is to move this system from the initial position $q(0)$ to the desired final position $q_d(T)$ in the time T with zero velocities on both ends.

3.1. Choice of q_m

Vector q could be written without loss of generality in the following way:

$$q = \begin{bmatrix} q_m \\ q_z \end{bmatrix} \tag{2}$$

where q_m has the same dimension as the rank of matrix B. Remaining z coordinates in vector q_z represents not directly actuated states, but this cannot be physically intuitively decided. This division of coordinates q is defined by the condition that the matrix B_m is the largest regular sub-matrix of the matrix B. According to the division of coordinates in (2) the equation (1) could be rewritten in the following form:

$$\begin{aligned} M^I_{mm}(q)\cdot\ddot{q}_m(t) + M^I_{mz}(q)\cdot\ddot{q}_z(t) &= F^I_m(q,\dot{q}) + B_m(q)\cdot u(t) \quad (3)\\ M^I_{zm}(q)\cdot\ddot{q}_m(t) + M^I_{zz}(q)\cdot\ddot{q}_z(t) &= F^I_z(q,\dot{q}) + B_z(q)\cdot u(t). \quad (4)\end{aligned}$$

There exists the inversion of the matrix B_m.

3.2. Elimination of u

Control input u can be derived from (3):

$$u(t) = B_m^{-1}(q)\cdot\left(M^I_{mm}(q)\cdot\ddot{q}_m(t) + M^I_{mz}(q)\cdot\ddot{q}_z(t) - F^I_m(q,\dot{q})\right). \quad (5)$$

Equation (5) is substituted into the equation (4) and results in:

$$\begin{aligned}&\left(M^I_{zm}(q) - B_z(q)B_m^{-1}(q)M^I_{mm}(q)\right)\cdot\ddot{q}_m(t)\\ &+\left(M^I_{zz}(q) - B_z(q)B_m^{-1}(q)M^I_{mz}(q)\right)\cdot\ddot{q}_z(t) = F^I_z(q,\dot{q}) - B_z(q)B_m^{-1}(q)F^I_m(q,\dot{q}).\end{aligned} \quad (6)$$

The dynamic system could be rewritten according to equations (3) and (6) as a new system:

$$M^{II}_{mm}(q)\cdot\ddot{q}_m(t) + M^{II}_{mz}(q)\cdot\ddot{q}_z(t) = F^{II}_m(q,\dot{q}) + B_m(q)\cdot u(t) \quad (7a)$$

$$M^{II}_{zm}(q)\cdot\ddot{q}_m(t) + M^{II}_{zz}(q)\cdot\ddot{q}_z(t) = F^{II}_z(q,\dot{q}) \quad (7b)$$

where

$$\begin{aligned} M^{II}_{mm}(q) &= M^I_{mm}(q)\\ M^{II}_{mz}(q) &= M^I_{mz}(q)\\ F^{II}_m(q,\dot{q}) &= F^I_m(q,\dot{q})\\ M^{II}_{zm}(q) &= M^I_{zm}(q) - B_z(q)B_m^{-1}(q)M^I_{mm}(q)\\ M^{II}_{zz}(q) &= M^I_{zz}(q) - B_z(q)B_m^{-1}(q)M^I_{mz}(q)\\ F^{II}_z(q,\dot{q}) &= F^I_z(q,\dot{q}) - B_z(q)B_m^{-1}(q)F^I_m(q,\dot{q}).\end{aligned}$$

Now the control input u is present only in the first equation of (7a) – (7b).

3.3. Exchange y and q_m

Let us consider such output y of the same dimension as the vector q_m

$$y = f(q) \quad (8)$$

that there exists such inversion of the function f, that the coordinates q_m can be uniquely determined from equation (8), so that

$$q_m = f^{-1}(y, q_z). \quad (9)$$

It is equivalent to the condition that rank of $\partial f/\partial q_m$ equals dimension of q_m in each position. One choice could be $y = q_m$ but for more general problems like the motion of flexible robot on the prescribed trajectory it is suitable to use the general relation (8).

Differentiating the equation (9) it is obtained

$$\begin{aligned} \dot{q}_m &= J_m\dot{y} + J_z\dot{q}_z \qquad (10)\\ \ddot{q}_m &= J_m\ddot{y} + J_z\ddot{q}_z + R(y,\dot{y},q_z,\dot{q}_z). \qquad (11)\end{aligned}$$

Next step is the substitution of $\ddot{q}_m, \dot{q}_m, q_m$ into the system of equations (7a) and (7b):

$$\begin{aligned} &M^{II}_{mm}(y,q_z)J_m\cdot\ddot{y} + \left(M^{II}_{mz}(y,q_z) + M^{II}_{mm}(y,q_z)J_m\right)\cdot\ddot{q}_z \\ &\quad = F^{II}_m(y,q_z,\dot{y},\dot{q}_z) - M^{II}_{mm}(y,q_z)R(y,\dot{y},q_z,\dot{q}_z) + B_m(y,q_z)\cdot u(t) \end{aligned} \qquad (12a)$$

$$M^{II}_{zm}(y,q_z)J_m\cdot\ddot{y} + \left(M^{II}_{zz}(y,q_z) + M^{II}_{mm}(y,q_z)J_m\right)\cdot\ddot{q}_z = F^{II}_z(y,q_z,\dot{y},\dot{q}_z). \qquad (12b)$$

By this way any desired output coordinates can be introduced. But the vectors $\ddot{y}, \dot{y}, y$ are renamed by $\ddot{q}_m, \dot{q}_m, q_m$ for convenience and there are created new matrices.

$$M_{mm}(q)\cdot\ddot{q}_m(t) + M_{mz}(q)\cdot\ddot{q}_z(t) = F_m(q,\dot{q}) + B_m(q)\cdot u(t) \qquad (13a)$$

$$M_{zm}(q)\cdot\ddot{q}_m(t) + M_{zz}(q)\cdot\ddot{q}_z(t) = F_z(q,\dot{q}) \qquad (13b)$$

where

$$\begin{aligned} M^{(13a)}_{mm}(q) &= M^{II}_{mm}(y,q_z)J_m\\ M^{(13a)}_{mz}(q) &= M^{II}_{mz}(y,q_z) + M^{II}_{mm}(y,q_z)J_m\\ F^{(13a)}_m(q,\dot{q}) &= F^{II}_m(y,q_z,\dot{y},\dot{q}_z) - M^{II}_{mm}(y,q_z)R(y,\dot{y},q_z,\dot{q}_z)\\ M^{(13b)}_{zm}(q) &= M^{II}_{zm}(y,q_z)J_m\\ M^{(13b)}_{zz}(q) &= M^{II}_{zz}(y,q_z) + M^{II}_{mm}(y,q_z)J_m\\ F^{(13b)}_z(q,\dot{q}) &= F^{II}_z(y,q_z,\dot{y},\dot{q}_z). \end{aligned}$$

There is necessary to ensure that matrix M_{zz} from the system of equations (13a)–(13b) is full rank. This system of equations is now used without loss of generality as the description of the system to be controlled.

3.4. Feedback linearization

The new input is chosen as w in order to linearize by feedback the system (13a):

$$\ddot{q}_m = w. \qquad (14)$$

Using equation (13b) it can be derived

$$\ddot{q}_z(t) = M^{-1}_{zz}(q)\cdot\left(F_z(q,\dot{q}) - M_{zm}(q)\cdot\ddot{q}_m(t)\right). \qquad (15)$$

Input torque is the function of w and its behavior comes from equations (13a), (14) and (15):

$$\begin{aligned} &\left(M_{mm}(q) - M_{mz}(q)M^{-1}_{zz}(q)M_{zm}(q)\right)\cdot\ddot{q}_m(t)\\ &\quad = F_m(q,\dot{q}) - M_{mz}(q)M^{-1}_{zz}(q)F_z(q,\dot{q}) + B_m(q)\cdot u(t) \end{aligned} \qquad (16)$$

$$\begin{aligned} u = B_m^{-1}(q)\left(M_{mm}(q) - M_{mz}(q)M_{zz}^{-1}(q)M_{zm}(q)\right)\cdot w \\ +B_m^{-1}(q)\left(M_{mz}(q)M_{zz}^{-1}(q)F_z(q,\dot{q}) - F_m(q,\dot{q})\right). \end{aligned} \tag{17}$$

Zero dynamics is in the following equation:

$$\ddot{q}_z(t) = M_{zz}^{-1}(q)\cdot\left(F_z(q,\dot{q}) - M_{zm}(q)\cdot w\right). \tag{18}$$

Using the input u from (17) the system (13a) – (13b) is transformed into the system (14) and (18).

3.5. How to get the new input w?

The question is, how to get a new input w to ensure that q_z ends in the desired position together with q_m. To find such w, which controls q_m is easy, but to find such w which controls q_m and q_z simultaneously is not trivial. The new input w contains two parts according to [8], it consists of the active part w_A which moves the q_m coordinates from the initial position $q_m(0)$ to the desired final ones $q_{md}(T)$ in time T from the equation (14) and the invariant part w_I which is invariant to the final position of the motion of q_m, but due to the dynamic connection through zero dynamics influences q_z in such a way that moves q_z from the initial positions $q_z(0)$ to the desired final ones $q_{zd}(T)$ in time T.

$$w = w_A + w_I. \tag{19}$$

The invariant w_I is such that

$$\begin{aligned} \int_0^T w_I \,\mathrm{d}t = 0 \\ \int_0^T\int_0^t w_I \,\mathrm{d}t\mathrm{d}t = 0. \end{aligned} \tag{20}$$

Substituting (19) into (14) and integrating the equation twice from $t = 0$ to $t = t$ it is obtained

$$\begin{aligned} \dot{q}_m(t) - \dot{q}_m(0) &= \int_0^t w_A \,\mathrm{d}t + \int_0^t w_I \,\mathrm{d}t \\ q_m(t) - q_m(0) &= \int_0^t\int_0^t w_A \,\mathrm{d}t + \int_0^t\int_0^t w_I \,\mathrm{d}t. \end{aligned} \tag{21}$$

Integrating now in the equations (21) from $t = 0$ to $t = T$ and using the first conditions (20) it is obtained

$$\begin{aligned} \dot{q}_m(T) - \dot{q}_m(0) &= \int_0^T w_A \,\mathrm{d}t + \int_0^T w_I \,\mathrm{d}t = \int_0^T w_A \,\mathrm{d}t \\ q_m(T) - q_m(0) &= \int_0^T\int_0^t w_A \,\mathrm{d}t + \int_0^T\int_0^t w_I \,\mathrm{d}t = \int_0^T\int_0^t w_A \,\mathrm{d}t. \end{aligned} \tag{22}$$

It is clear that the motion of q_m in the final velocity and position is influenced only by the active part w_A of the control (19). This control is chosen arbitrarily just for the

fulfillment of the desired final values of position and velocity of q_m. When the active part w_A is chosen, it is a given function of time $w_A(t)$ and substitution of (19) into (18) results into

$$\ddot{q}_z(t) = M_{zz}^{-1}(q) \cdot (F_z(q, \dot{q}) - M_{zm}(q) \cdot (w_A(t) + w_I)) \,. \tag{23}$$

Now the motion of q_z can be controlled by the choice of w_I just fulfilling the conditions (20). For the invariant motion it is used so-called natural motions and its frequencies f_i,

$$w_I = \sum_i A_i \sin(2\pi f_i t + \Phi_i) \tag{24}$$

where amplitudes A_i and phases Φ_i are some constants as a result of optimization. The frequencies f_i are chosen and the amplitudes A_i and phases Φ_i are optimized in order the coordinate q_z reaches the desired position and velocity at the chosen settling time.

If it holds

$$2\pi f_i T = 2K_i \pi \tag{25}$$

for some natural number K_i, then the functions (24) satisfy the conditions (20). How to determine suitable frequencies is explained in the next section.

4. NATURAL MOTION

The natural motion is the motion of the investigated mechanical system moving in the gravity field with zero or constant inputs (drive torques), usually from the unstable equilibrium position to the stable equilibrium position. To reach the desired quiescent motion, it is necessary to add passive members (dampers) into the positions of actuators. Underactuated part moves freely, but due to the overall energy flow into the passive parts, it stabilizes around the equilibrium point. The damping term (added passive members) is chosen small just in order to take out the difference of potential energy between the equilibrium positions. The value of the damping term is optimized with respect to the settling time. Later they are important just the eigenfrequencies of the natural motion and they are not influenced by the damping if it is small. The frequencies must be the eigenfrequencies in order to excite the system sufficiently.

During the simulation all states are recorded. Designed feedforward control is constructed from this natural motion.

The eigenfrequencies of the natural motion describe the vibrational motion of the variables q that ends at the equilibrium where all swings meet at the final time. Therefore the conditions (25) are satisfied. On the other side in fact the determined eigenfrequencies are rational numbers and therefore the natural numbers K_i at the final time T for any set of eigenfrequencies f_i exist. Finally the conditions (25) from the natural motion are to be satisfied just approximately in order to move the mechanical system into such vicinity of the upper equilibrium that the NQR control can stabilize the motion.

The excitation of the system at its eigenfrequencies enables to cause large motion of the system based on resonance. Therefore the Fourier analysis of the natural motion is applied in order to determine the eigenfrequencies of the nonlinear system under consideration. The eigenfrequencies allows exciting the mechanism with less input energy than other frequencies as the excitation by eigenfrequencies enables to accumulate the energy in the system.

The system is nonlinear and the determination of the eigenfrequencies is not easy. Therefore the usage of natural motion is helpful.

5. SIMULATION OF DOUBLE INVERTED PENDULUM

On the Figure 2 it is the scheme of double inverted pendulum.

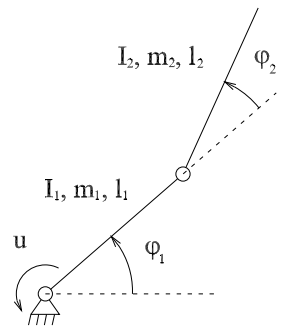

Fig. 2. Scheme of double inverted pendulum with coordinates, parameters and torque.

It consists of two links and one actuator placed between the first link and the base frame. Using Lagrange equations of the second type the dynamic equations of double inverted pendulum (26) can be formulated according to the equations (13a) and (13b).

$$M = \begin{bmatrix} I_2 + \frac{m_2 {l_2}^2}{4} + \frac{m_2 l_1 l_2 \cos(\varphi_2)}{2} & I_1 + I_2 + m_2 l_1 (l_1 + l_2 cos(\varphi_2)) + \frac{m_1 {l_1}^2 + m_2 {l_2}^2}{4} \\ I_2 + \frac{m_2 {l_2}^2}{4} & I_2 + \frac{m_2 {l_2}^2}{4} + \frac{m_2 l_1 l_2 cos(\varphi_2)}{2} \end{bmatrix}$$

$$F = \begin{bmatrix} m_2 l_1 l_2 \sin(\varphi_2)(\frac{\dot{\varphi}_2^2}{2} + \dot{\varphi}_1 \dot{\varphi}_2) - g\frac{m_2 l_2}{2}\cos(\varphi_1 + \varphi_2) - g l_1 (\frac{m_1}{2} + m_2)\cos(\varphi_1) \\ -m_2 l_1 l_2 \sin(\varphi_2)\frac{\dot{\varphi}_1^2}{2} - g\frac{m_2 l_2}{2}\cos(\varphi_1 + \varphi_2) \end{bmatrix}$$

$$M(\varphi_2) \begin{bmatrix} \ddot{\varphi}_2 \\ \ddot{\varphi}_1 \end{bmatrix} = F(\varphi_1, \dot{\varphi}_1, \varphi_2, \dot{\varphi}_2) + u(t) \begin{bmatrix} 1 \\ 0 \end{bmatrix}. \tag{26}$$

These equations are immediately in the form (13a) and (13b). Matrix M in (26) is inertia matrix and vector F contains forces dependent on velocities and external forces besides the control inputs. Actuator u is rotational element acting between the base frame and the first link. It is chosen that φ_1 corresponds to q_z and φ_2 to q_m from equation (2). The matrix B_m from (13a) equals one and M_{zz} from the equation (13b) equals $I_2 + \frac{m_2 {l_2}^2}{4} + \frac{m_2 l_1 l_2 \cos(\varphi_2)}{2}$, which must be nonzero and for chosen parameters it is. The sequence of variables in the state vector is chosen to fit with the system of equations (13a) and (13b).

Based on the physical intuition the φ_1 is actuated and should be equal to q_m. But based on the system of equations (3) – (4) it is an arbitrary choice the splitting of q into q_m and q_z upon the fulfillment that B_m is full rank and subsequently M_{zz} is full rank. Based on the results of [8] it is suitable (powerful) to control the motion of the

underactuated system by the control of the intuitively not actuated variable (here φ_2) as the motion of the system is more sensitive to its motion.

In our case φ_1 was chosen as q_z and φ_2 as q_m. The choice could be changed into φ_1 as q_m and φ_2 as q_z based on the first equation in (26).

For the simulation the following parameters are used: inertia of the first and second link is 0,1 kg, their moments of inertia are 0,01 kg/m^2 and length of each part is 1 m with the center of gravity in the middle of each part.

Natural motion is illustrated in Figure 3. The natural motion is achieved by the simulation of the equations of motion (26) with zero control and damping instead of it, $u(t) = -b \cdot \dot{\varphi}_1$ from the upper position to the lower position. The outer line represents end point of the second link, inner dotted line is trajectory of the first link. It starts in upper position with a little deflection in the first angle φ_1 and zero velocities. It falls down into the bottom stable position with quiescent motion. This behavior is caused by damping force acting between the first link and the base frame, where the actuator is later placed. The damping coefficient ($b = 0.357$Nms/rad) is received by optimization with respect to the settling time. The behavior of whole states including accelerations is recorded.

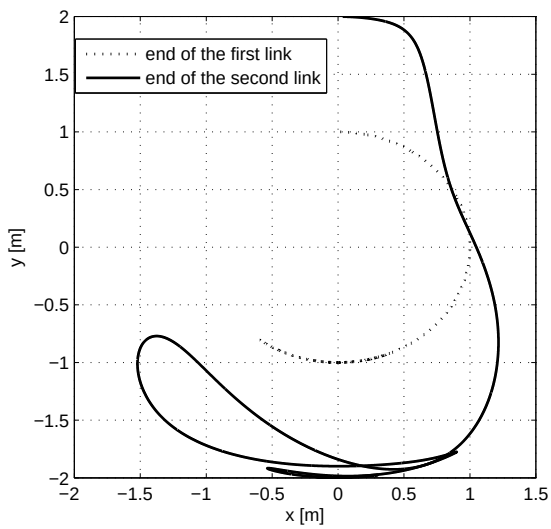

Fig. 3. Motion of double pendulum from its upper position into the bottom position with damping between the first link and the base frame.

The behavior of double inverted pendulum was obtained and now it is used to design the control of the system. It is necessary to apply exact input-output feedback linearization to use data from the natural motion of the pendulum. Second derivative of coordinate φ_2 is selected as a new control variable w (which corresponds to the equation (14)). The remaining coordinate φ_1 could be expressed directly from the equation (26)

and the zero dynamics (see corresponding equation (18)) is the equation (27b).

$$\ddot{\varphi}_2 = w \tag{27a}$$

$$\ddot{\varphi}_1 = \frac{F_2 - M_{22} \cdot w}{M_{21}} \tag{27b}$$

where

$$M = \begin{bmatrix} M_{11} & M_{12} \\ M_{21} & M_{22} \end{bmatrix}$$

$$F = \begin{bmatrix} F_1 \\ F_2 \end{bmatrix}.$$

The singular positions corresponding with the Figure 1 are for the $\varphi_2 = \pm\pi/2$ and other states zero. The system of equations (27a) – (27b) get the following form:

$$\begin{aligned} \ddot{\varphi}_2 &= w \\ \ddot{\varphi}_1 &= w \end{aligned} \tag{28}$$

where both links are moving in the same manner, control can't distinguish between links and becomes singular. The equation (28) shows just the singular position of the mechanism at some points and proofs the uncontrollability.

The expression for actuator u is according to (17) following:

$$u(t) = \frac{M_{11}F_2 - M_{21}F_1 - \det(M) \cdot w}{M_{21}}. \tag{29}$$

Data from the natural fall down motion are used now. First frequencies from the first link angular acceleration create the basis for the new input variable for swing-up motion (Figure 4).

Input variable w consists of active and invariant part (according to equation (19)). In this case active part is zero, because variable φ_2 has the same initial and final position. Sinusoidal behavior of invariant part has frequencies from the first link movement, because w directly influences φ_1 through zero dynamics in equation (27b). Amplitudes are proportional to the difference in potential energy between initial and final mechanism position, but their value is the result of optimization.

$$E_p = m_1 l_1 g + m_2(2l_1 + l_2)g. \tag{30}$$

All parameters and behavior of the control variable w are in the equation (31).

$$\begin{aligned} A &= \begin{bmatrix} \frac{m_1 \cdot g \cdot l_1 + m_2 \cdot g \cdot (2l_1 + l_2)}{2} & \frac{m_1 \cdot g \cdot l_1 + m_2 \cdot g \cdot (2l_1 + l_2)}{4} \end{bmatrix} \\ \Phi &= \begin{bmatrix} -\frac{\pi}{2} & \frac{\pi}{2} \end{bmatrix} \\ f &= \begin{bmatrix} 0,38147 & 0,85831 \end{bmatrix} \\ \ddot{\varphi}_2 &= w \\ w_A &= 0 \\ w_I &= \sum_{i=1}^{2} A_i \cdot \sin(2\pi \cdot f_i \cdot t + \Phi_i) \\ w &= w_A + w_I. \end{aligned} \tag{31}$$

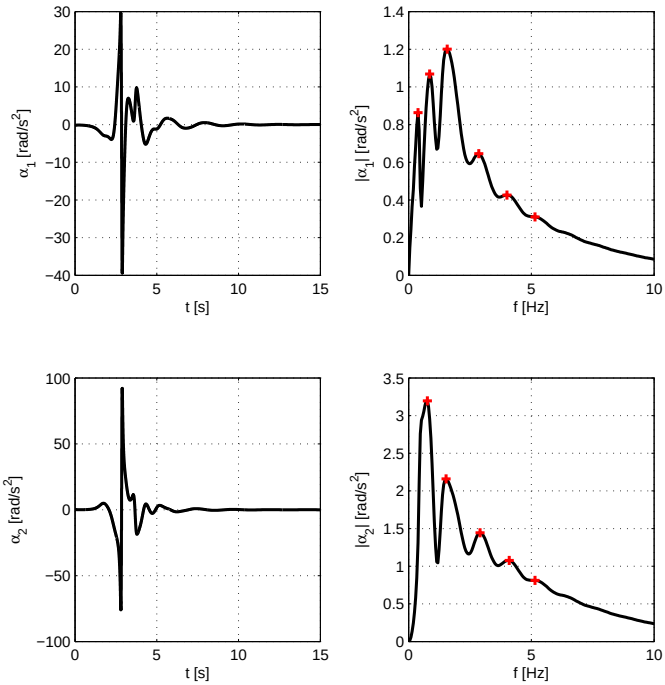

Fig. 4. Accelerations (left) and its Fourier transformations. Frequencies for the first link angular acceleration are: 0.38147, 0.85831, 1.5736, 2.861, 4.0054 and 5.1498 Hz and frequencies for the second link angular acceleration: 0.76294 (= 2 × 0.38147), 1.5259, 2.9087, 4.1008 and 5.1498 Hz.

Because the control near the upper position is switched to the NQR, the condition (25) is fulfilled only approximately, but it holds $T = \frac{4}{f_1} = \frac{9}{f_2} = 10.48575\,\mathrm{s}$, $K_1 = 4,\ K_2 = 9$. It is interesting that the frequencies determined from the natural motion (see Figure 4) satisfies the artificial invariant condition (25). The usage of these frequencies is probably efficient because they are the eigenfrequencies and the system is sensitive to the input on these frequencies.

Simulated swing-up motion guided by relative angular acceleration $\ddot{\varphi}_2 = w$ between the first and the second link described in the equation (31) reaches the unstable equilibrium position (see Figure 5) and it is necessary to switch to another stabilizing controller nearby the upper unstable position.

The control algorithm NQR controls the system from the position in the surrounding of the upper unstable position to this unstable equilibrium. But the region of attractivity of this control is also limited. It could be found that for the system under consideration

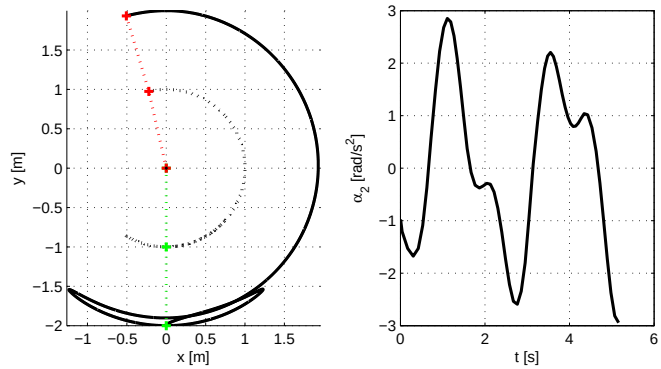

Fig. 5. Swing-up motion controlled by angular acceleration; left mechanism end points in the working plane, right input angular acceleration behavior.

the controllability matrix in NQR algorithm is independent on relative angular velocity of the second link but it is dependent on the angular position of the both links and quite strictly on the angular velocity of the first link. The controller NQR calculates every time step the input torque u at the first link. Therefore the input variable u is plotted in the same figure based on the angular acceleration (29) and based on the NQR algorithm in the vicinity of the unstable equilibrium.

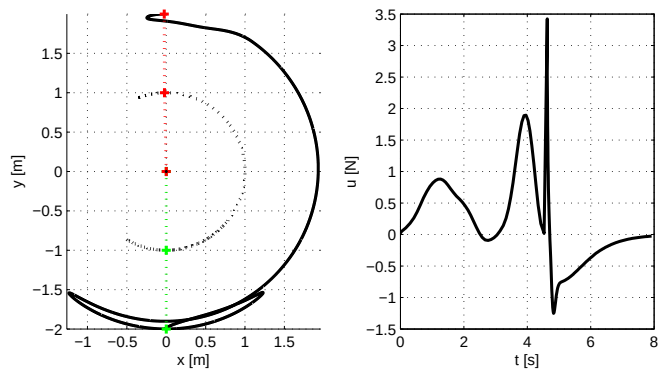

Fig. 6. Final swing up motion for double pendulum; left motion in the plane, right input torque acting on the first link.

The control algorithm NQR starts at time 4.72 s. There is visible big step in the input torque when changing between the control strategies on the Figure 6, left. For the illustration you can see on the Figure 7 behavior of φ_1 and φ_2 coordinates and their velocities.

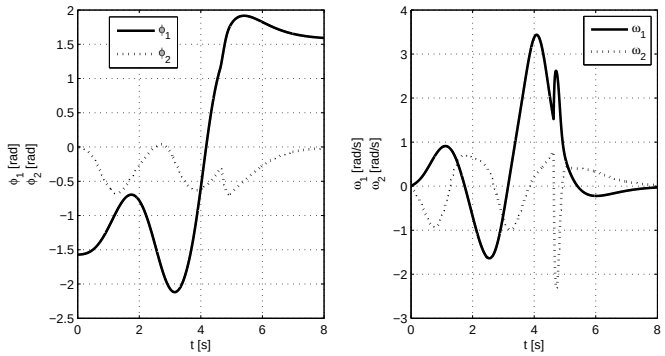

Fig. 7. Upwards movement of double inverted pendulum, angular positions and velocities.

6. SIMULATION OF INVERTED PENDULUM

The same approach has been applied to the inverted pendulum on the cart, see the Figure 8.

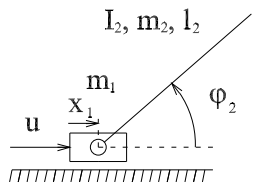

Fig. 8. Inverted pendulum with coordinates, parameters and acting force.

This mechanism consist of the cart moving horizontally, the link rotationally connected with the cart and there is a force acting on the cart. The following dynamic equations are obtained using Lagrange equations of the second type.

$$M = \begin{bmatrix} m_1 + m_2 & -m_2 l_2 \sin(\varphi_2) \\ -m_2 l_2 \sin(\varphi_2) & I_2 + m_2 {l_2}^2 \end{bmatrix}$$

$$F = \begin{bmatrix} m_2 l_2 \cos(\varphi_2)\dot{\varphi}_2^2 \\ -g m_2 l_2 \cos(\varphi_2) \end{bmatrix}$$

$$M(\varphi_2) \begin{bmatrix} \ddot{x}_1 \\ \ddot{\varphi}_2 \end{bmatrix} = F(x_1, \varphi_2, \dot{x}_1, \dot{\varphi}_2) + u(t) \begin{bmatrix} 1 \\ 0 \end{bmatrix}. \tag{32}$$

These equations (32) are also immediately in the form (13a) and (13b). Matrix M in (32) is inertia matrix and vector F contains forces dependent on velocities and external forces besides the control inputs. The coordinate φ_2 corresponds to q_z and x_1 to q_m

from the equation (2). The matrix B_m from the equation (13a) equals one and M_{zz} from the equation (13b) equals $I_2 + m_2 {l_2}^2$, which is nonzero. Actuator u is transversal force element acting on the cart.

Simulation parameters are: the weights are 0.1 kg and 0.1 kg for the cart and pendulum respectively, the moment of inertia of the pendulum is 0.01 kg/m^2 and the pendulums' length is 1 m.

Natural motion of the pendulum with the cart is on the Figure 9. The natural motion is achieved by the simulation of the equations of motion (32) with zero control and damping instead of it, $u(t) = -b \cdot \dot{x}_1$ from the upper position to the lower position. It starts with pendulum slightly deflected from the upper position with zero velocities and falls down due to the gravity to the bottom equilibrium position. Damping force takes effect on the cart as horizontal force and the damping coefficient ($b = 0.79147$ Ns/m) is received by optimization with respect to the settling time. All states including accelerations are recorded.

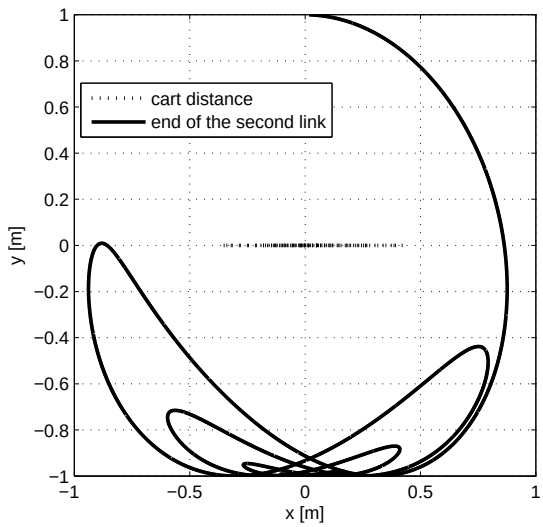

Fig. 9. Motion of inverted pendulum with damping between cart and base frame. Outer line represents movement of the ending point of the link.

From the behavior of the pendulum on the cart it is designed the control of the system. Exact input-output linearization is applied and as a new control variable is selected $\ddot{x}_1$, because the inertia matrix M from the equation (11) is not suitable for using the $\ddot{\varphi}_2$ as a control variable – for the φ_2 equals zero or straight angle, in the zero dynamics according to the equation (18) is division by zero. In this particular case it is possible to use directly actuator u as a new input. The $\ddot{\varphi}_2$ is derived from the equation

(32) and represents zero dynamics (see equation (18)).

$$\ddot{x}_1 = w \tag{33a}$$

$$\ddot{\varphi}_2 = \frac{F_2 - M_{21} \cdot w}{M_{22}} \tag{33b}$$

where

$$\begin{aligned} M &= \begin{bmatrix} M_{11} & M_{12} \\ M_{21} & M_{22} \end{bmatrix} \\ F &= \begin{bmatrix} F_1 \\ F_2 \end{bmatrix}. \end{aligned}$$

The singular positions corresponding with the Figure 1 are for the $\varphi_2 = [0, \pi]$ and other states zero. The system of equations (33a) – (33b) get the following form:

$$\begin{aligned} \ddot{x}_1 &= w \\ \ddot{\varphi}_2 &= \frac{F_2}{M_{22}} \end{aligned} \tag{34}$$

where control variable can't influence the link and control becomes singular. The singular position of the mechanism at some points is shown in the equation (34) and proofs the uncontrollability.

The expression for actuator u is according to (17) following:

$$u(t) = \frac{M_{12}F_2 - M_{22}F_1 + \det(M) \cdot w}{M_{22}} \tag{35}$$

The behavior of new control variable $\ddot{x}_1$ is based on the angular acceleration of the pendulum, because $\ddot{x}_1$ directly influences $\ddot{\varphi}_2$ through the zero dynamics (equation (33b)). The control variable has two parts (according to equation (19)), zero active part and invariant part with sinusoidal shape having the frequencies taken from the angular acceleration of the pendulum during the natural motion. From the frequency content of the angular acceleration are taken first two frequencies (Figure 10).

Amplitudes are proportional to the potential energy needed to move the link from the lower position into the upper stable position, the value used for control is the result of optimization.

$$E_p = 2l_2 \cdot g \cdot m_2. \tag{36}$$

All parameters and overall equation for the control variable w are in (37).

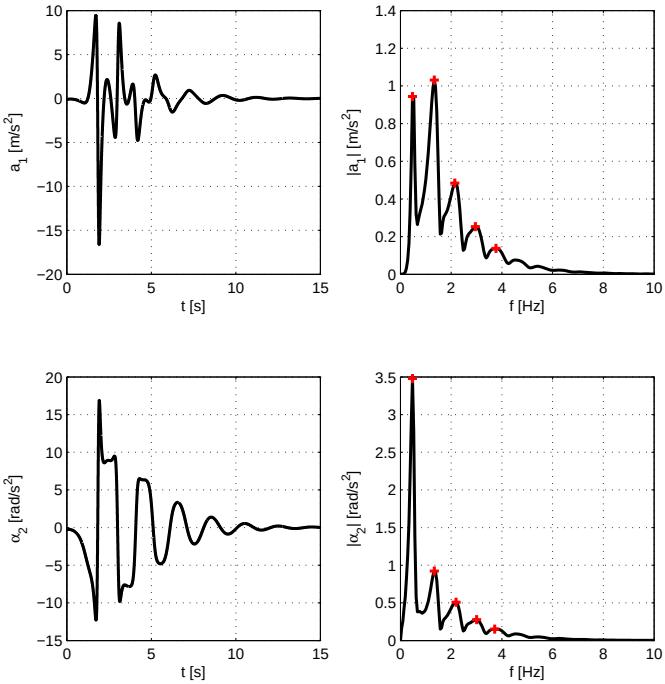

Fig. 10. Accelerations (left) and its Fourier transformations. Frequencies for the cart acceleration are: 0.47684, 1.3351, 2.1458, 2.9564 and 3.767 Hz and frequencies for the link angular acceleration: 0.47684, 1.3351, 2.1935, 3.0041 and 3.7193 Hz.

$$
\begin{aligned}
A &= \left[\begin{array}{cc} 6 \cdot 2l_2 \cdot g \cdot m_2 & 3 \cdot 2l_2 \cdot g \cdot m_2 \end{array}\right] \\
\Phi &= \left[\begin{array}{cc} -\frac{\pi}{2} & \frac{\pi}{2} \end{array}\right] \\
f &= \left[\begin{array}{cc} 0,47684 & 1,3351 \end{array}\right] \\
\ddot{x}_1 &= w \\
w_A &= 0 \\
w_I &= \sum_{i=1}^{2} A_i \cdot \sin(2\pi \cdot f_i \cdot t + \Phi_i) \\
w &= w_A + w_I
\end{aligned} \tag{37}
$$

The condition (25) is fulfilled only approximately because the control near the upper position is switched to NQR, but it holds $T = \frac{5}{f_1} = \frac{14}{f_2} = 10.48575\,\mathrm{s}$, $K_1 = 5$, $K_2 = 14$.

The motion of mechanism which is controlled by new input variable w is on the Figure 11. The mechanism is passing by the desired position (see Figure 11 left) and for the stabilization around the upper equilibrium it is necessary to use the local stabilization control. This motion is driven by sinusoidal force unlike damping force acting during fall down motion on the Figure 9, so these (fall down and upwards) are two different motions, therefore trajectories in Figure 9 and Figure 11 are different.

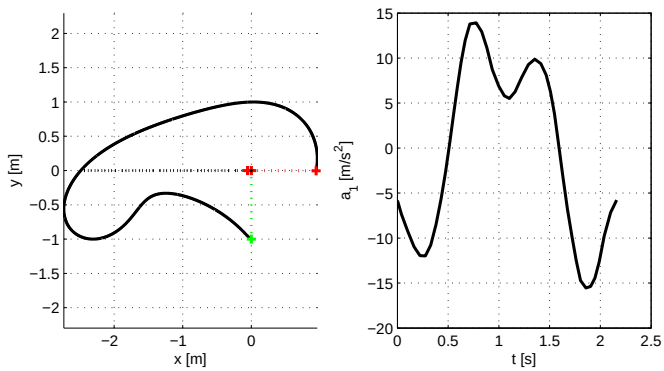

Fig. 11. Swing-up motion controlled by cart acceleration; left mechanism and right input cart acceleration behavior.

Stabilization of the system around the equilibrium is achieved by the NQR controller. When the pendulum reaches the point, where it is controllable by NQR, it is switched on and it leads the mechanism to the equilibrium. The control algorithm NQR starts at 1.98 s. The entire trajectory of the end point of the pendulum and cart is on the Figure 12 left, with starting and final position marked. On the Figure 12 right is the behavior of the input force acting on the cart. There is one big peak in the force when changing from the feedforward control to the NQR feedback control.

The pendulum and cart movements are displayed on Figure 13.

7. CONCLUSIONS

This paper has presented a new control of underactuated mechanical systems using inspiration from natural motion of these mechanisms. This control method uses the exact input-output feedback linearization. It demonstrates the method for finding the trajectory going through singular positions. It is based on the falling trajectory (natural motion) and on the trajectory constructed using the eigenfrequencies of this motion. The method is applied to the double inverted pendulum and to the pendulum on the cart (cart-pole system). For the feedforward control strategy the first two frequencies are used taken from the natural motion. The calculated amplitudes correspond to the energy needed for the system to change its potential energy in the field of gravity. Another new fact is that the zero dynamics included in the underactuated mechanisms could be controlled by frequencies added to the signal of the control variable.

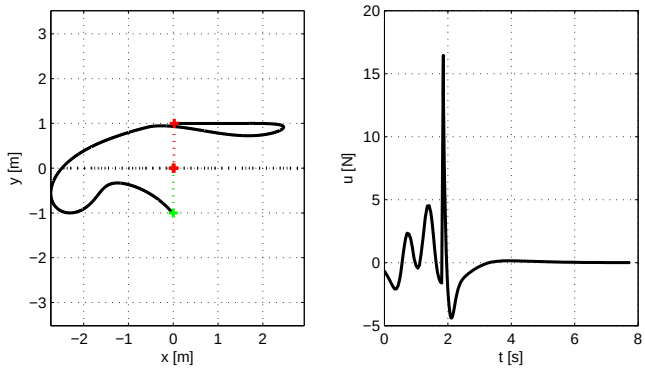

Fig. 12. Final swing up motion of the cart with pendulum.

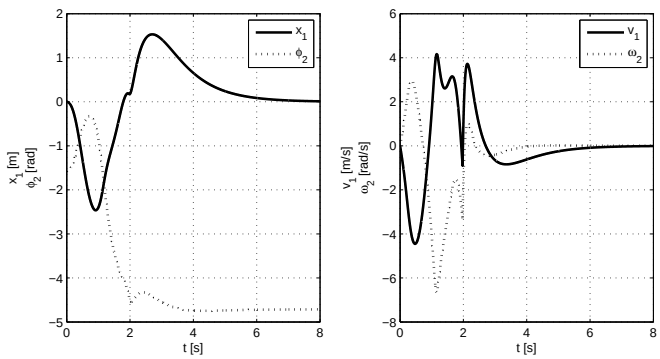

Fig. 13. Position and speed of cart and angular position and speed of pendulum behavior during the swing-up motion.

There is a large potential to extend this approach into the field of underactuated systems for feedforward control passing singular positions and to stabilize the unwanted movements of the flexible structures. Next goal is to develop control theory for mechanisms without any potential field.

ACKNOWLEDGEMENT

This work was partially supported by the project 'Algorithms for computer simulation and application in engineering' MSM 6840770003.

(Received March 29, 2011)

REFERENCES

[1] N. P. I. Aneke: Control of Underactuated Mechanical Systems. Ph.D. Thesis. Technische Universiteit Eindhoven, Eindhoven 2002.

[2] I. Fantoni and R. Lozano: Non-linear Control for Underactuated Mechanical Systems. Springer–Verlag, London 2002.

[3] A. D. Mahindrakar, S. Rao, and R. N. Banavar: A Point-to-point control of a 2R planar horizontal underactuated manipulator. Mechanism and Machine Theory *41* (2006), 838–844.

[4] R. Olfati-Saber: Nonlinear Control of Underactuated Mechanical Systems with Application to Robotics and Aerospace Vehicles. Ph.D. Thesis. Massachusetts Institute of Technology, Boston 2001.

[5] J. Rubí, Á. Rubio, and A. Avello: Swing-up control problem for a self-erecting double inverted pendulum. IEE Proc. – Control Theory App. *149* (2002), 2, 169–175.

[6] P. Steinbauer: Nonlinear Control of the Nonlinear Mechanical Systems. Ph.D. Thesis. Czech Technical University in Prague, Prague 2002. (in Czech)

[7] L. Udawatta, K. Watanabe, K. Izumi, and K. Kuguchi: Control of underactuated robot manipulators using switching computed torque method: GA based approach. Soft Computing *8* (2003), 51–60.

[8] M. Valášek: Control of elastic industrial robots by nonlinear dynamic compensation. Acta Polytechnica *33* (1993), 1, 15–30.

[9] M. Valášek: Design and control of under-actuated and over-actuated mechanical systems – Challenges of mechanics and mechatronics. Supplement to Vehicle System Dynamics *40* (2004), 37–50.

[10] M. Valášek: Exact input-output linearization of general multibody system by dynamic feedback. In: Multibody Dynamics 2005, Eccomas Conference, Madrid 2005.

[11] M. Valášek and P. Steinbauer: Nonlinear control of multibody systems. In: Euromech Colloquium 404, Advances in Computational Multibody Dynamics, Lisboa: Instituto Suparior Technico Av. Rovisco Pais, 1999, 437-444.

Zdeněk Neusser, Czech Technical University, Technická 4, 166 07 Praha 6. Czech Republic.
e-mail: Zdenek.Neusser@fs.cvut.cz

Michael Valášek, Czech Technical University, Technická 4, 166 07 Praha 6. Czech Republic.
e-mail: Michael.Valasek@fs.cvut.cz